SERI/TP-217-3342
UC Category: 261
DE88001166

Preliminary Results from the Dynamic Response Testing of the Northern Power Systems 100-kW Wind Turbine

R. M. Osgood
S. M. Hock

June 1988

Prepared for IECEC 1988
Denver, Colorado
1 August, 1988

Prepared under Task No. WE811202

Solar Energy Research Institute
A Division of Midwest Research Institute
1617 Cole Boulevard
Golden, Colorado 80401-3393

Prepared for the
U.S. Department of Energy
Contract No. DE-AC02-83CH10093

Printed in the United States of America
Available from:
National Technical Information Service
U.S. Department of Commerce
5285 Port Royal Road
Springfield, VA 22161

Price: Microfiche A01
Printed Copy A02

Codes are used for pricing all publications. The code is determined by the number of pages in the publication. Information pertaining to the pricing codes can be found in the current issue of the following publications, which are generally available in most libraries: *Energy Research Abstracts, (ERA); Government Reports Announcements* and Index (*GRA* and I); *Scientific and Technical Abstract Reports (STAR)*; and publication, NTIS-PR-360 available from NTIS at the above address.

Preliminary Results from Dynamic Response Testing of the Northern Power Systems 100-kW Wind Turbine

R.M. Osgood
S.M. Hock

Solar Energy Research Institute
Wind Research Branch
1617 Cole Boulevard
Golden, CO 80401

Abstract

The Solar Energy Research Institute (SERI), in cooperation with Northern Power Systems (NPS), conducted a series of dynamic response tests on the NPS 100kW Wind Turbine as part of the Department of Energy's (DOE) Cooperative Field Test Program. This paper presents a preliminary review of the test data, including average and cyclic machine response characteristics. The mean turbine operating conditions are analyzed as a function of mean wind speed and rotor azimuth position using the method of bins. Rotor bending loads are also presented in the frequency domain to investigate the relative effects of low- and high-frequency wind turbulence.

Introduction

As part of the DOE Cooperative Field Test Program, SERI and NPS conducted a series of tests designed to characterize the dynamic response of the 100-kW NPS Wind Turbine. The machine was located on the Souza Ranch property in Altamont Pass, California. An extensive array of anemometers was located directly upwind of the turbine to provide detailed information on the wind inflow. Preliminary results indicate that the machine operating parameters are close to those predicted by the designers.

Turbine Description

The NPS 100-kW "North Wind 100" wind turbine has a two-bladed, upwind, teetered rotor employing an innovative rotor control system. The 17.8-m diameter rotor is composed of two fiberglass blades and is located at a hub height of 25.6 m, atop a tapered steel tubular tower. The turbine has been designed to maximize energy production over a wide range of wind regimes by employing a dual speed, double generator configuration. Power production begins at a cut-in wind speed of 3.3 m/s, and rated power is reached at 14 m/s.

The rotor control system is a passive hydraulic system with full blade pitch control. This design concept uses the wind forces and the inertial forces inherent in the moving rotor to automatically change the blade pitch to control turbine output power.

The yaw system employs both a passive self-aligning yaw system with a yaw drive for backup. The yaw drive system is a helical-bevel gear motor engaged at the yaw bearing. The yaw drive system is used to align the rotor upwind of the tower in light winds and prior to turbine operation. However, the turbine is designed to be operated in free yaw upwind of the tower during normal operation.

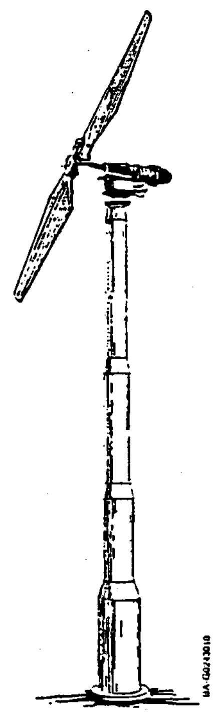

Figure 1. Northern Power Systems 100-kW "North Wind 100"

The drive train can be considered as two subsystems, mechanical and electrical. The mechanical portion is composed of a Flender two-stage, two-speed gearbox with a one-way sprag clutch. It produces high-speed, 1800-rpm output from the low-speed shaft inputs of 72-rpm and 48-rpm. The electrical part of the drive train consists of two fully enclosed induction generators. The first generator is rated at 25-kW for the low-speed 48-rpm mode of operation, and the second is rated at 100-kW for the 72-rpm mode.

Test Description and Instrumentation

The test turbine, shown in Figure 1, was located at the peak of a ridge which runs perpendicular to the predominant wind direction.

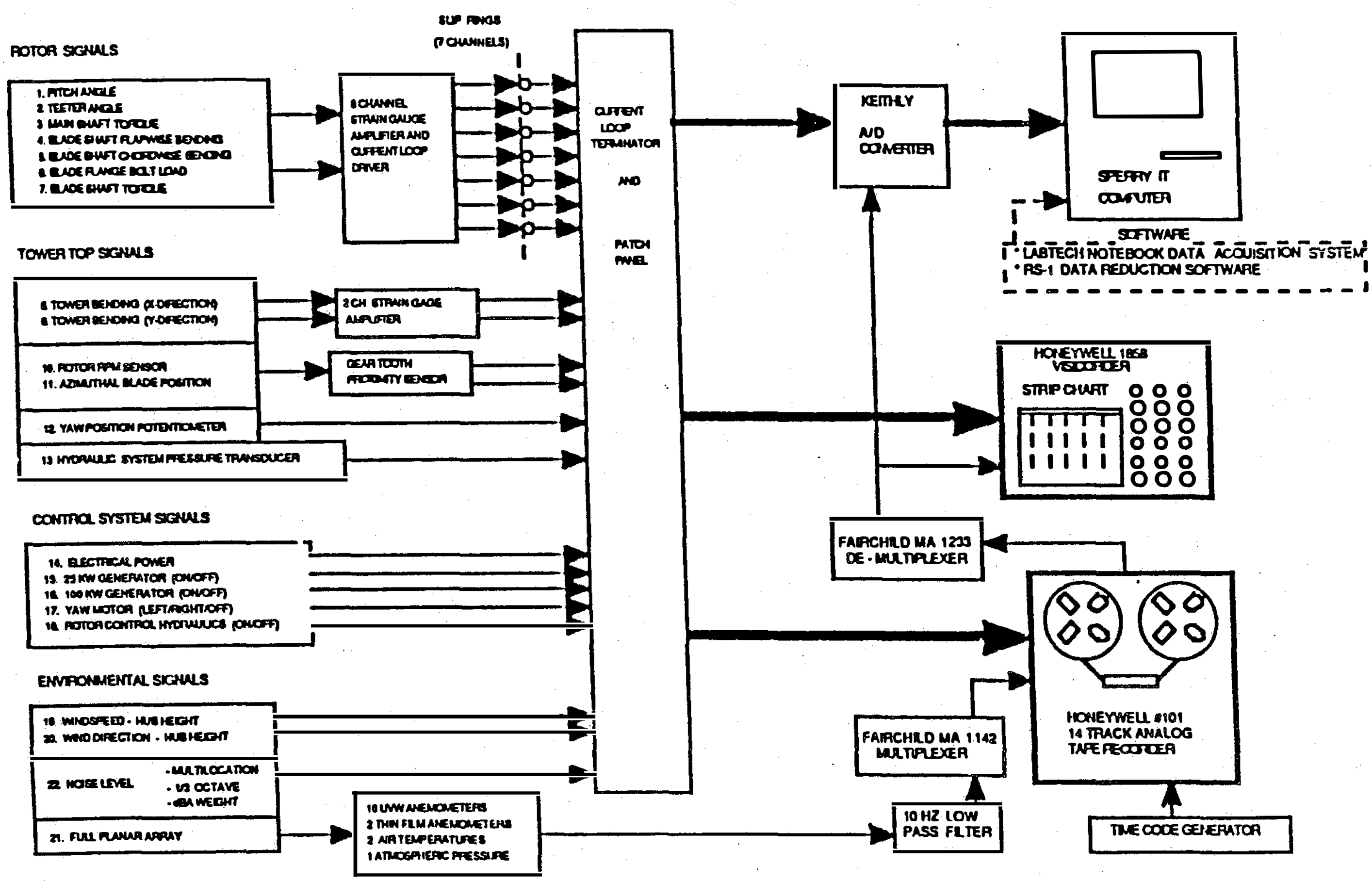

Figure 2. Dynamic Response Test Instrumentation Schematic

The surrounding terrain consists predominantly of rolling hills. The estimated annual average wind speed for this site is 6.9 m/s.

The dynamic response testing was carried out during the 1987 wind season (late summer and fall) after an intensive effort to install the instrumentation and anemometry. The test program objectives were to acquire and document the operating loads and performance parameters of the turbine, and provide a detailed view of the wind characteristics for correlation with the loads and performance data. Extensive instrumentation on the rotor and turbine, as well as an array of anemometers located upwind of the rotor, provided the required data.

In all, 82 channels of data were fed into the test trailer where they were multiplexed and stored on a 16-track magnetic tape for later analysis. The test engineers also had the capability to examine the data real time, as selected channels could be displayed on strip chart recorders or a spectrum analyzer, or could be fed into the SERI midscale data acquisition system. The quick-look midscale data acquisition system was comprised of a Keithley digitizer that fed data into a desktop computer using Labtech Notebook software. The selected data channels could then be displayed real time or stored on a disk. Figure 2 presents a schematic of the test instrumentation setup.

For this preliminary analysis, a limited number of channels were selected to provide insight into the turbine's operation. Table 1 lists the 12 channels discussed in this paper.

The machine operating data were filtered at 10 Hz, and the anemometer data were filtered at 1 Hz; both were digitized at a sample rate of 37 Hz at SERI on the NEFF 720 system. This high sample rate allows the resolution needed to resolve the rotor angular position for azimuthal averaging. The wind speed and direction data were collected from a meteorological tower located approximately two rotor diameters upwind of the wind turbine.

Table 1. Selected Channels for Initial Analysis.

Channel #	Description
1	Blade #1 root flap-bending moment
2	Blade #1 pitch angle
3	Teeter angle
4	Low-speed shaft torque
5	Blade #1 root chord-bending moment
6	Yaw angle
7	Rotor Azimuth angle
8	Generator power
9	Wind speed at 11.0 m
10	Wind speed at 20.7 m
11	Wind speed at 36.5 m
12	Wind direction at 20.7 m

Study Data Cases

The recorded data spans the full range of wind speeds from 2 m/s to 23 m/s. We tabulated statistics based on 10-min records for selected channels, which were used to characterize the data base. From this table, we were able to select six 10-min cases based on the operating conditions. These cases represent a range of mean wind speeds from 16 m/s to 33 m/s, and turbulence intensities (standard deviation of wind speed divided by the mean) from low turbulence at 0.09 to very high turbulence at 0.20. Table 2 summarizes these conditions, as well as generator power output.

The variation of wind speed vertically across the rotor is shown in Figure 3. The wind shear profiles appear to vary dramatically from

SERI

Table 2. **Operating Conditions for the Six 10-min Data Cases.**

Data Case #	Disk Average Wind Speed (m/s)	Turbulence Intensity	Power Output (kW)
1	27.2	0.14	36.6
2	33.0	0.09	69.3
3	29.3	0.15	79.4
4	32.1	0.10	93.6
5	29.1	0.12	78.8
6	16.0	0.20	25.1

case to case. Case #6 represents a large negative shear, and the other cases have smaller positive shears. Most of the curves tend to have a knee at the middle height, with the slopes often reversing. This could be because the meteorological tower with the anemometers is located near the top of a steep rise, which may be accelerating the flow.

One selection criterion for each case was that the wind direction was within ± 10 degrees from the alignment between the turbine and the meteorological tower. Thus, the flow passing through the anemometers should also pass through the rotor disk plane to give the best possible correlation between wind inputs and turbine response. The wind data for this paper were collected from propvane anemometers located 27 m upwind of the turbine.

Data Analysis

Three different statistical approaches were applied to the data for each of the six cases. First, the mean turbine responses were computed using the method of bins. Second, azimuth averaging was used to isolate the deterministic portion of the time-series turbine responses. Finally, the means were removed from the blade-bending loads and spectral analysis was used to look at the frequency characteristics of the loads.

Mean Turbine Responses

The per-revolution averaged turbine responses of blade-bending moments, power, teeter, and pitch angles were binned as a function of disk averaged wind speed. The preaveraging over the time period of one rotor revolution was used to eliminate the higher harmonic responses. The disk averaged wind speed was simply the mean of the three anemometers, where each of the anemometer signals was also preaveraged over a period of one rotor revolution. The turbine responses were binned into 0.5 mps bins, and bins containing less than ten data points were discarded. No density correction or pressure adjustments were made to the data.

Figure 4 shows the per-revolution averaged system power output binned versus wind speed for the six data cases. It also shows the point where the system operation is switched from the low speed mode of 48-rpm to the high-speed mode of 72-rpm. Data cases 1 and 2 appear to stand out from the rest. This can be explained from the pitch angle settings, which for cases 1 and 2 are much higher at 13° than for the other data cases, which are between 8° and 10°. For those two data cases, the hydraulic pressure for the blade pitch control was, in fact, manually set lower to limit peak power production for testing purposes.

The higher blade pitch angle for data cases 1 and 2 also affected the mean blade flapwise bending moments, as shown in Figure 5. The theoretical root flap-bending moment for a blade pitch angle of 2° is included in Figure 5 for reference. The general trend of higher loads under increasing wind speed is readily apparent.

Deterministic Turbine Responses

It is assumed that for stationary operating conditions of the test turbine the deterministic and stochastic loads can be separated by the process of azimuth averaging. Azimuth averaging is accomplished by binning the measured forces with respect to the azimuth angle of the rotor blade for a large number of rotor cycles. The results of this averaging process are signals that are

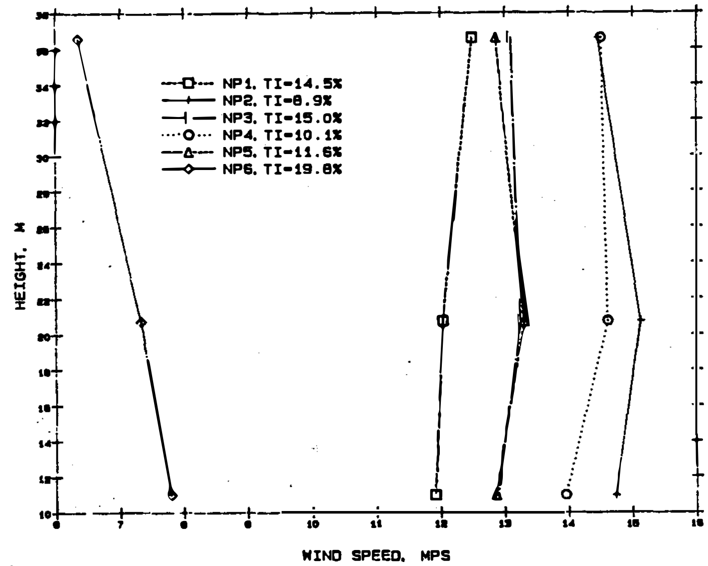

Figure 3. Ten-Minute Average Wind Speed Profiles

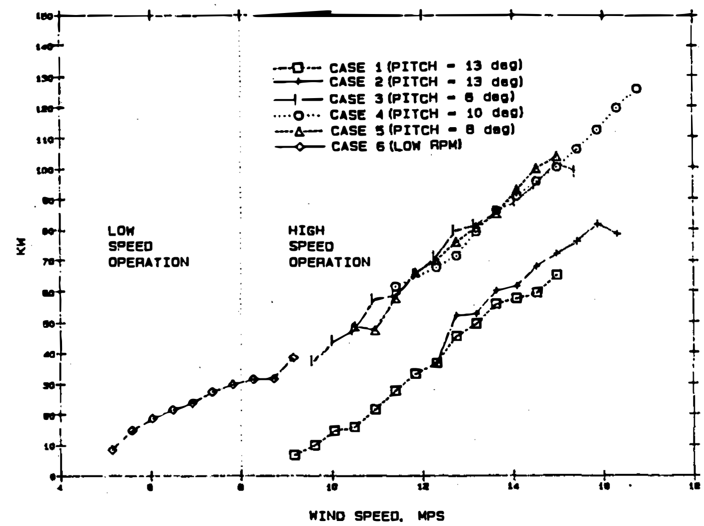

Figure 4. Per-Revolution Averaged System Power

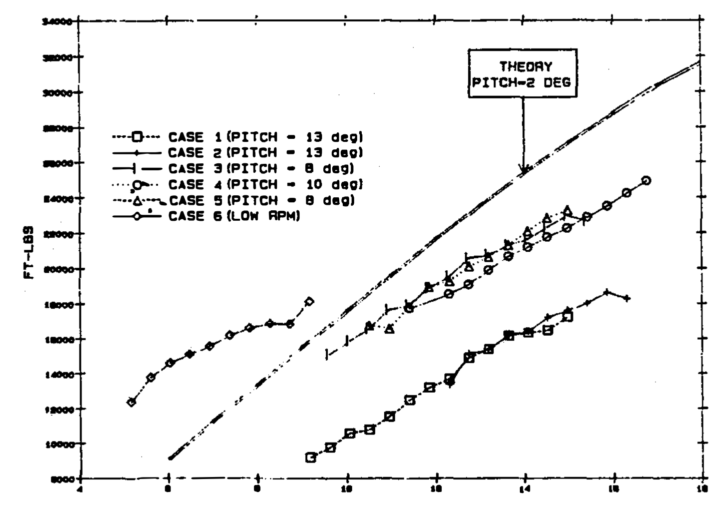

Figure 5. Per-Revolution Averaged Root Flapwise Bending Moment

periodic with rotor angle and provide an estimate of the deterministic forces acting over the averaging time.

The time-series rotor bending moments were binned on blade azimuth signal for each ten-min data case to produce the azimuth-averaged plots shown in Figures 6 and 7. Figure 6 contains the azimuth averaged root flapwise bending moments for data cases 1-6. As can be seen in Figure 6, all six cases have the same characteristic waveform, with only a change in the mean levels. A blade position of 0° represents the blade pointing straight up, so 180° corresponds to straight down. As expected, the bending loads peak near 90° (blades horizontal), which is typical of a teetered rotor. In this position, the teetering acceleration is a maximum, producing higher bending moments due to inertial loads. The teetering motion is excited by the wind shear and a gravity moment for nonzero blade pitch angles. In order to enhance upwind yaw stability, teeter springs were used to provide a stronger wind-following moment from the rotor. This accounts for the dominant one-per-revolution bending-moment fluctuation seen in Figure 6, rather than the expected two-per-revolution response for a freely teetering rotor. Case 6 has a strong negative wind shear, as shown in Figure 1; this translates to a lower-amplitude cyclic bending moment, as the azimuth averaged plot clearly shows.

Figure 7 contains the azimuth averaged root chordwise bending moment for data cases 1-6. The dominant contributor to this load is the weight of the blade as it rotates; thus, the characteristic waveform peaks as the blade passes through a horizontal position, and the force of the blade weight is perpendicular to the blade. This strong one-per-revolution load is dominant for every data case.

Another interesting signal to observe in the azimuth averaged format is the rotor teeter angle, shown in Figure 8. The shape of this signal changes more dramatically between data cases, as it is heavily dependent on the wind inflow to the rotor. For higher wind shears, the peak-to-peak, one-per-revolution amplitude of the teeter angle increases, as in data cases 3 and 4. It is clear that higher-order teeter responses are also affected, as is the phase angle; however, the correlation of this signal to the wind input in terms of wind shear and turbulence intensity has not yet been determined. It is possible that this could also be affected by the vertical component of the wind, which needs to be investigated further.

Frequency Content of Blade-Bending Loads

In order to further investigate the higher harmonics of the blade-bending loads, the time series data were transformed to the frequency domain. The root flapwise and chordwise bending moments are presented in power spectral density plots in Figures 9 and 10 for data case 4. The linear trends were first removed from the time series data in an attempt to reduce the DC component of the signals; however, these plots represent the stochastic or random part of the bending moments as well as the deterministic portion. Data case 4 represents the highest overall wind speed with the blade pitch in the normal run position.

Some of the harmonics of the blade passage frequency are indicated in Figures 9 and 10 and are labeled 1P and 2P. The spectral plots clearly identify these frequencies with narrow spectral peaks. These portions of the signal are probably the deterministic rotor responses. The broader spectral peaks near the natural frequencies are mostly the rotor responses to turbulence excitation. The first symmetric flapwise mode is indicated by a broad peak around 3.25 Hz, and the second symmetric flapwise mode is shown by a peak around 9.0 Hz in Figure 9. The same tendencies can be seen in the chordwise-bending-moment power spectral density plot of Figure 10. Here the first symmetric chordwise mode is shown at 4.3 Hz. The chordwise signal indicates the presence of higher-order deterministic responses, as indicated by the narrow spikes, clearly evident up to the 8P mark in Figure 10.

Another interesting feature of the spectral density plots is the relative contribution to the energy in the bending moments between the low- and high-frequency portions of the signal. Even

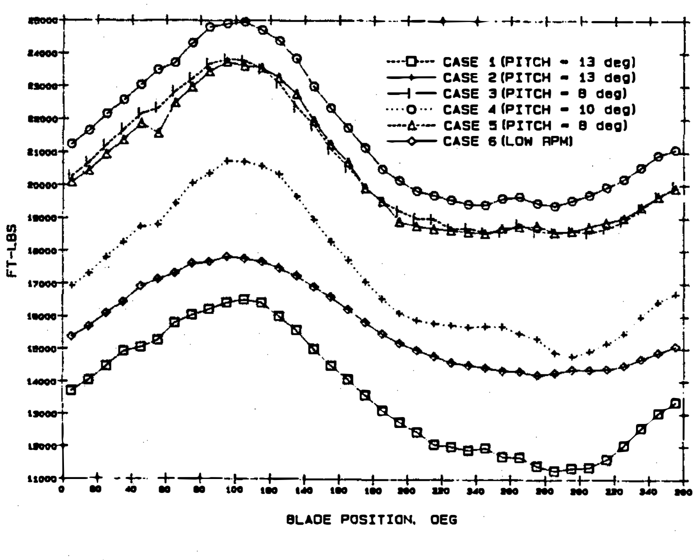

Figure 6. Azimuth Averaged Root Flapwise Bending Moment

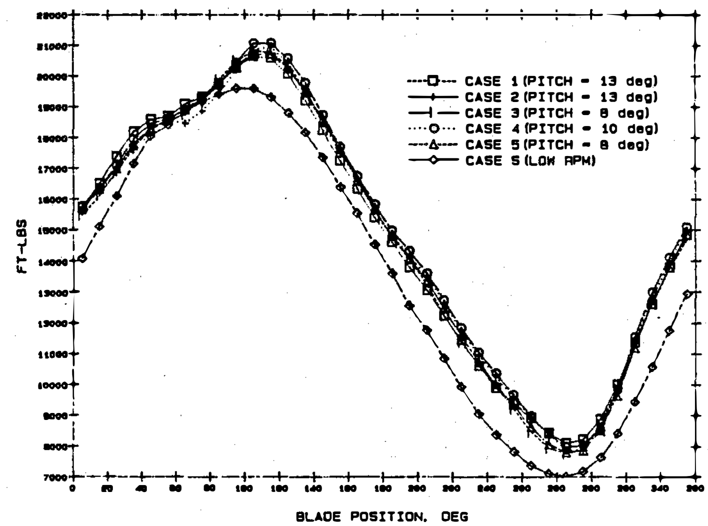

Figure 7. Azimuth Averaged Root Chordwise Bending Moment

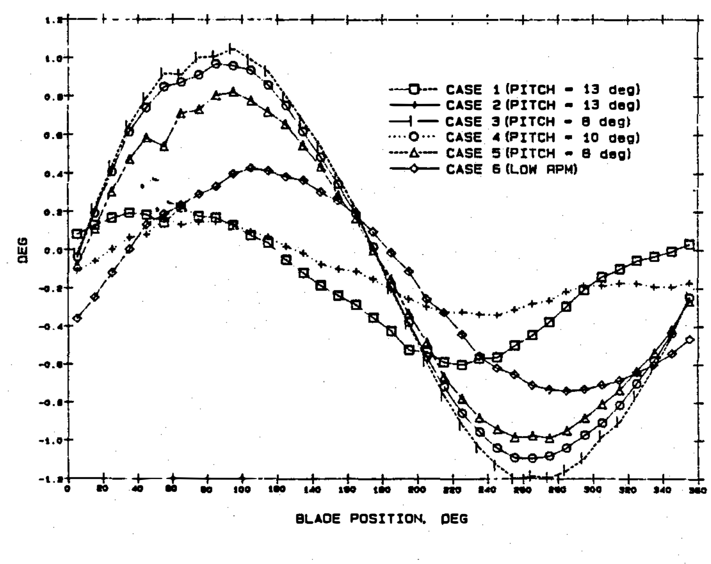

Figure 8. Azimuth Averaged Teeter Angle

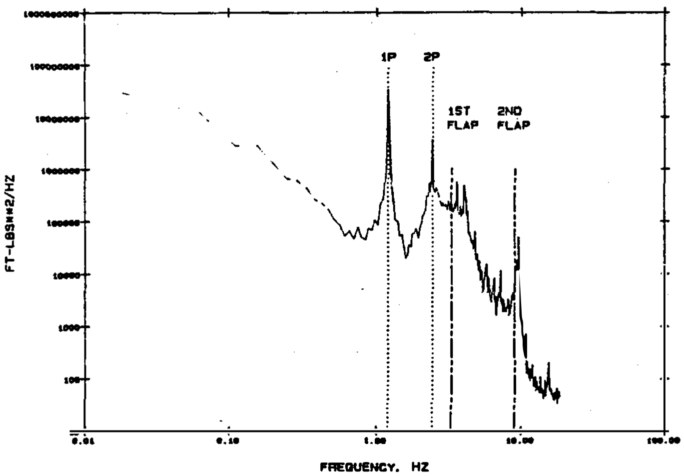

Figure 9. Power Spectral Density Plot of Blade Root Flapwise Bending Moment for Data Case 4

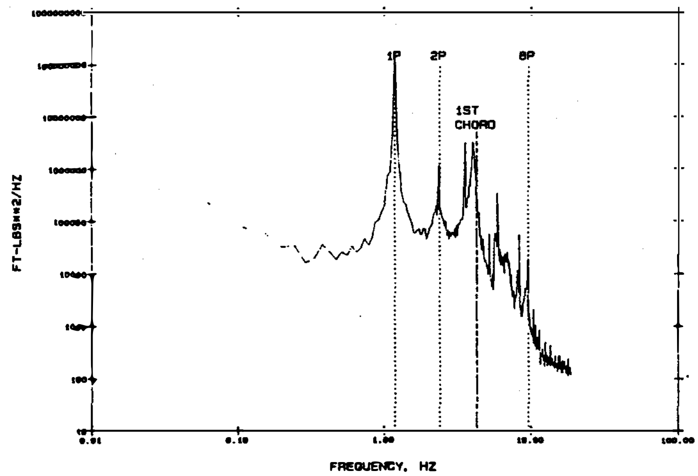

Figure 10. Power Spectral Density Plot of Blade Root Chordwise Bending Moment for Data Case 4

with the linear trend removed, the energy in the low-frequency part of the flapwise bending moment is significant compared to the higher-frequency contributions. There appears to be less low-frequency content in the chordwise bending moment signal, which is expected, because it is dominated by the one-per-revolution gravity loading.

Conclusions

The six selected ten-min data cases from the dynamic response testing of the NPS 100-kW wind turbine have been examined using three different analyses. The binning analysis defined the mean turbine operating states. The method of pre-averaging over one rotor revolution and averaging three anemometers gave results consistent with design characteristics.

Azimuth averaging characterized the deterministic signals by effectively filtering out the stochastic response. The signals obtained this way showed a smooth transition of waveform with wind speed. The root-bending moments were also analyzed in the frequency domain, after the linear trends were removed. This analysis allowed the key rotor responses to be identified and indicated that the stochastic contributions to the cyclic loads are highest at frequencies well below one-per-revolution. The bending responses at the blade natural frequencies are quite subdued with overall response levels two orders of magnitude below the low-frequency maximum. This demonstrates this teetering rotor's relatively benign response to turbulence in the inflow.

Acknowledgments

This work was sponsored by the United States Department of Energy under contract number DE-AC02-83CH10093. The authors wish to acknowledge the assistance of Ed McKenna and Jack Allread of the SERI Wind Research Branch's instrumentation group. Brian McNiff, Clint Coleman, and Steve Hamblin from Northern Power Systems also provided significant contributions to the test project.

References

1. Coleman, Clint, and McNiff, Brian: "Final Report, Dynamic Response Testing of the 'North Wind 100' Wind Turbine Generator," draft, Northern Power Systems, PO Box 556, Moretown, VT 05674. December 1987.